Waveguide effect under 'antiguiding' conditions in graded anisotropic media

2010 J. Phys.: Condens. Matter 22 075401

(http://iopscience.iop.org/0953-8984/22/7/075401)

J. Phys.: Condens. Matter **22** (2010) 075401 (11pp) doi:10.1088/0953-8984/22/7/075401

Waveguide effect under 'antiguiding' conditions in graded anisotropic media

A V Kozlov, V G Mozhaev and A V Zyryanova

Faculty of Physics, Moscow State University, Moscow, 119991 GSP-1, Russia

E-mail: av_kozlov@inbox.ru, vgmozhaev@mail.ru and annazyr@mail.ru

Received 11 November 2009, in final form 8 January 2010
Published 29 January 2010
Online at stacks.iop.org/JPhysCM/22/075401

Abstract
A new wave confinement effect is predicted in graded crystals with a concave slowness surface under conditions of growth of the phase velocity with decreasing distance from the waveguide axis. This finding overturns the common notion about the guiding and 'antiguiding' profiles of wave velocity in inhomogeneous media. The waveguide effect found is elucidated by means of ray analysis and particular exact wave solutions. The exact solution obtained for localized flexural waves in thin plates of graded cubic and tetragonal crystals confirms the predicted effect. Since this solution is substantially different with respect to the existence conditions from all others yet reported, and it cannot be deduced from the previously known results, the predicted waves can be classified as a new type of waveguide mode in graded anisotropic media. Although the concrete calculations are given in the article for acoustic waves, its general predictions are expected to be valid for waves of various natures, including spin, plasma, and optical waves.

1. Introduction

Material science is one of the high priority scientific areas at the present time. Among various new materials, functionally graded ones attract a great deal of attention as promising for application in a variety of technical and scientific fields [1]. These spatially inhomogeneous materials are characterized by a gradual variation in composition and structure over their volume that allows the production of parts and components with specified properties. The study of the wave properties of such materials is important for both fundamental and practical reasons, in particular, for material characterization and non-destructive testing. Waveguide phenomena in different inhomogeneous media have been studied for a long time by many researchers for waves of various natures, including seismic, acoustic and optical waves, radio and plasma waves, spin waves, gravity-capillary waves, and some others (see, for example [2–12]). For smoothly inhomogeneous isotropic media, it is now firmly established that the waveguide localization occurs in regions near the minimum phase velocity [13]. As an alternative and equivalent formulation of this 'waveguide law', the requirement of a decrease of the index of refraction with increasing distance from the waveguide axis is frequently mentioned in the literature [14]. In particular, it is stated in a monograph [15] that 'a necessary condition for guiding the optical wave is that the refractive index of the cladding is lower than that of the core . . .. In the graded index fiber, the refractive index is maximum on the axis and decreases towards the cladding region'. Such guiding media are also called lens-like or focusing ones. On the other hand, the regions of maximum wave velocity are known as 'antiguiding' [13, 16]. The refraction leads to wave rays bending and pushing away from these regions, forming shadow zones where no direct rays from a point source occur. No exceptions to these 'waveguide laws' are known as yet. However the anisotropy effect on these common 'waveguide laws' in smoothly inhomogeneous media such as crystals has not been addressed yet. Note that localized states and excitations in both crystalline and non-crystalline solids are of importance in the study of various dynamic processes [17, 18].

Among the various anisotropies of material properties of condensed matter, the simplest is the ellipsoidal one. A mere change of scale of the ellipsoid axes transforms the ellipsoidal characteristic surfaces (which are entirely convex) into spheres. This is a simple and direct way to generalize the known formulae and solutions of the isotropic case to the case of media with ellipsoidal anisotropy. Such anisotropy is typical, for example, for optical waves in homogeneous dielectric crystals [19], because their anisotropic properties are determined by the second-rank tensors of dielectric

permittivity and magnetic susceptibility. Media with local concavities on the characteristic surfaces have much more complicated anisotropic wave properties. Local concavities of the slowness surfaces are common for electromagnetic waves in plasma [20, 21], spin waves in ferromagnetics [22], optical waves in photonic crystals [23] and acoustic waves in anisotropic solids [24], and these concavities can be the cause of new wave effects. One such effect is predicted and studied theoretically in the present paper under the combined conditions of anisotropy and spatial inhomogeneity of material properties. Namely, it is shown below that a smooth decrease, rather than the commonly assumed growth of acoustic wave phase velocity with increasing distance from the waveguide axis, can lead to waveguide localization in crystals with locally concave slowness surfaces. It is pertinent to point out that this velocity profile corresponds to conditions which are 'antiguiding' for both isotropic [13, 16] and anisotropic media with convex slowness surfaces. Thus, the predicted effect is due to specific anisotropy, and so it is in principle impossible in isotropic media.

A partial waveguide localization, i.e. localization with energy leakage, may, in general, occur in the regions of maximum phase velocity in the media with discontinuities of wave characteristics, such a high-velocity layer inserted in or lying on a low-velocity medium [25]. If the impedance ratio of these two materials is large enough, this produces strong reflections at the interfaces. Then the waves excited in such a high-velocity layer travel over long distances with multiple reflections and relatively low energy loss per reflection at the interface, resulting in a partial waveguide effect. However, from the mathematical point of view it is just a pseudo-localization since the outer wave field of leaky modes radiated from the waveguide, with rare exception [26], is not localized in space. This topic is beyond the scope of the present paper where only true waveguide localization without leakage is analyzed.

Concerning our interest in the problem under discussion, it can be mentioned that two of us have recently studied the effect of a narrow thin liquid layer on the waveguide localization of surface acoustic waves (SAW) on piezoelectric substrates. The first attempt to investigate this problem was made ignoring the substrate anisotropy [27]. A further account of the anisotropy has shown that it can enhance the SAW localization, and this enhancement is especially strong in the case when the curvature of the SAW slowness curve in the vicinity of the propagation direction tends to zero [28]. However, that analysis belongs to the case of entirely convex slowness curves, while the consideration of locally concave slowness curves in the present paper leads to the prediction of a novel uncommon waveguide phenomenon.

2. Elliptical and hyperbolic wave models

In general all material properties can vary over the volume of graded materials. On the other hand, in some multicomponent anisotropic media the relative variations of the elastic stiffnesses with component content can be much less than those of the mass density. This case occurs, for example, in cubic crystals of $Al_xGa_{1-x}As$ with a varying content, x, of Al [29]. Therefore, the account of only the mass density spatial dependence and ignoring that for stiffnesses might be both a good approximation and a considerable simplification of the problem for such media. This simplified model of anisotropic graded media is used further for analytical studies in the present paper. A similar model was used in [30] for ray tracing in anisotropic inhomogeneous medium with a linear velocity gradient when the elastic properties vary only by a simple scale factor. As an additional simplification, we assume that the mass density depends only on the distance from the waveguide axis, which is considered to be parallel to a symmetry axis of the graded crystals.

The case of strict elliptical anisotropy is realized for pure shear acoustic waves propagating in the crystal mirror plane and polarized perpendicularly to this plane. For waves polarized along the Z axis and propagating in the XY mirror plane in crystals, with X being the symmetry axis, and with constant mass density, the equation of motion has the form

$$\rho\ddot{u}_z = C_x\frac{\partial^2 u_z}{\partial x^2} + C_y\frac{\partial^2 u_z}{\partial y^2}. \tag{1}$$

Here u_z is the displacement component, $C_x = c_{55}$ and $C_y = c_{44}$ are the elastic stiffnesses, ρ is the mass density. Equation (1) remains unchanged when ρ is a function of the transverse coordinate y. If this function is even, it may be approximated by a parabolic dependence

$$\rho = \rho_0(1 - \gamma_2 y^2), \tag{2}$$

where ρ_0 and γ_2 are constant. Since the mass density should obviously be positive, equation (2) can only be used if $|y| \leqslant 1/\sqrt{\gamma_2}$ for $\gamma_2 > 0$. This known defect of the parabolic approximation [31] can be excluded in another model of graded media for which ρ and C_y are considered constant while $C_x = C_{x0}(1 + \tilde{\gamma}_2 y^2)$, and where C_{x0} and $\tilde{\gamma}_2$ are constant.

The hyperbolic anisotropy cannot be exact for acoustic waves. Nevertheless, it can be used as an approximation of the local concavity of the slowness curve in the direction of wave propagation. The equation of motion for this model has the same general form as equation (1) with the only difference being the sign of the coefficient C_y, which is negative in the hyperbolic case. The basis for considering such a case is the possibility to derive equation (1) for quasi-shear waves in the paraxial approximation [32], since the effective elastic constant C_y for these waves becomes negative when a concavity of the slowness curve appears near the x axis. Further, the two cases of elliptical and hyperbolic anisotropies, which differ only in the sign of C_y, are considered as one.

Searching for the solution in the form of harmonic waves with angular frequency ω, $u_z = u_0(y)\exp(\mathrm{i}k_x x - \mathrm{i}\omega t)$, reduces equation (1) to an ordinary differential equation which looks like the Schrödinger equation for a quantum harmonic oscillator

$$\frac{\partial^2 u_z}{\partial y^2} + (p - \alpha^2 y^2)u_z = 0, \tag{3}$$

where $p = (k_0^2 - k_x^2)/A$, $\alpha^2 = k_0^2\gamma_2/A$, $A = C_y/C_x$, $k_0^2 = \rho_0\omega^2/C_x$. Under the condition

$$p = (2n + 1)\alpha, \qquad n = 0, 1, 2, \ldots, \tag{4}$$

equation (3) has the known localized solutions

$$u_z^n = u_{z0}^n \exp(-\xi^2/2) H_n(\xi) \exp(\mathrm{i}k_x^n x - \mathrm{i}\omega t), \qquad (5)$$

where $\xi = y\sqrt{\alpha}$, k_x^n is the propagation constant of the nth mode defined by equation (4), u_{z0}^n is the mode amplitude, H_n is a Hermite polynomial of order n, $H_n(\xi) = (-1)^n \exp(\xi^2)\frac{\mathrm{d}^n \exp(-\xi^2)}{\mathrm{d}\xi^n}$.

It should be noted that the same equation as (3) has been used in [28] for the analysis of the anisotropy-induced increase of beam compression of guided Rayleigh waves. However, for the Rayleigh waves this is only an approximate model equation rather than an exact one as it is for the shear waves. In addition, the effect of concavity of the slowness curves, which is the focus of the present study, has not been considered in the mentioned paper. An intriguing property of the anisotropic solution (5) noticed in [28] is the superstrong compression of the waveguide beams in the limit $\alpha \to \infty$, when the anisotropy parameter A becomes infinitely small. In this case the curvature of the slowness surface near the X axis tends to zero. It is important to stress here that both equation (1) for a medium with variable mass density and its solution (5) are exact for pure shear waves. Thus, the conclusion on waveguide beam compression when the slowness surface curvature decreases is absolutely reliable and correct for waves of this type. However, the pure elliptical anisotropy makes it practically impossible to achieve the limit of zero curvature. The strongest known compression of the slowness ellipse for pure shear waves is found in tellurium dioxide crystals in the plane with normal (110) [33]. But even in this case the ellipse eccentricity is no more than 3.4. This is illustrated in figure 1, where subscripts of the slowness projections denote the corresponding crystallographic directions. Both the real and imaginary branches of the slowness curve for that case are presented. These branches are calculated as solutions to the secular equation in the case when the varying horizontal slowness projection is real. Note that both the real and imaginary (or complex) branches of the slowness curves are of interest for the analysis of various wave phenomena [34–37]. Hereafter, the slowness projections are normalized by their value corresponding to wave propagation along the horizontal axis. In this form of representation, the slowness surfaces are identical to the iso-frequency surfaces in wavenumber space.

Let us now discuss the effect of the slowness concavity on the solution (5). If the convex slowness model is replaced by the concave one, the imaginary hyperbolic branch shown by the dashed line in figure 1 becomes real. For that, it is necessary to change the signs of C_y and, consequently, of A. Since, according to the formula for α, the localized modes exist only if the signs of the coefficients A and γ_2 are the same, γ_2 should also change its sign in this case. Thus, in contrast to the common situation that occurs for the convex slowness, the guiding velocity profile for the concave slowness should be inverse (at least, in this simplified hyperbolic model), i.e. the velocity should decrease rather than grow with increasing distance from the waveguide axis. This prediction is further supported by a ray analysis.

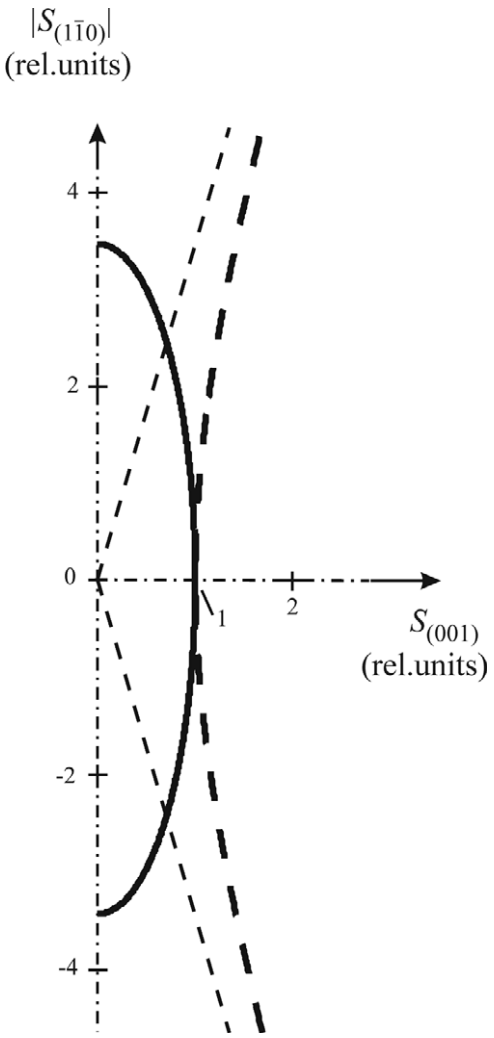

Figure 1. Real and imaginary branches of the slowness curve (S) for pure shear waves, propagating in the (110) plane of tellurium dioxide. The real branch is given by the full line. The oblique straight dashed lines are the asymptotics for the hyperbolic imaginary branch given by the dashed curve. The slowness projections are normalized by the value corresponding to wave propagation along the horizontal axis.

3. Ray theory

Ray analysis is a simple and illustrative method allowing a better understanding of wave phenomena and so it could be useful for the physical explanation of the predicted, uncommon and paradoxical, at first view, waveguide effect. Such an approach is used in this section to elucidate the mechanism of wave localization in anisotropic media with 'antiguiding' velocity profiles. Note that the ray constructions were previously carried out for inhomogeneous media with elliptic anisotropy and various velocity profiles (see, for example [9, 10, 30, 38, 39]), but the case of waveguides with parabolic velocity profile was studied only for isotropic media [8].

A common ray path corresponding to localized waveguide modes propagating along the horizontal axis X is shown in figure 2. The construction of rays for this path at different distances from the waveguide axis is demonstrated

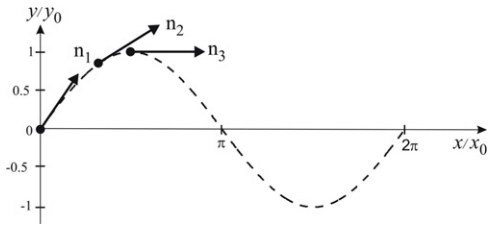

Figure 2. Typical wave ray path for guided modes. The coordinate y_0 corresponds to the ray turning point, x_0 is the ray period. Three selected rays are depicted: n_1 at the waveguide axis, n_3 at the turning point, n_2 at an intermediate distance.

in figures 3(a) and (b), in both cases of convex and concave slowness surfaces. For this Snell's law is used, according to which the tangential projections of the refracted wavevectors and, consequently, of the slownesses are continuous as the wave rays propagate in inhomogeneous media. It follows, from the solution presented in section 2, that if $A > 0$, the slowness of the waveguide modes is less than the local horizontal slowness at the waveguide axis. For wavenumbers this means that $k_x < k_0$, where k_0 is defined above and can be interpreted as the propagation constant for wave rays lying on the waveguide axis and traveling along this axis. The inequality between k_x and k_0 in the solution found is reversed in the concave slowness case when $A < 0$. These inequalities prescribe the admissible fixed (according to the Snell's law) horizontal projections of the slowness, indicated for selected localized modes by dashed vertical lines in figures 3(a) and (b). The crossings of the vertical lines with the slowness curves, drawn at different distances from the waveguide axis, determine the corresponding vertical slowness projections. In turn, the normals n_1, n_2 and n_3 to the curves constructed at the crossing points in figures 3(a) and (b) define the directions of the wave rays, like those shown in figure 2. The general shape of the slowness surface in the particular case under study is not changed as the rays move from the waveguide axis, since only the mass density varies, being a simple scale factor for the slowness. So, its cross-sections, corresponding to the wave rays shown in figures 3(a) and (b), differ from each other only in scale rather than form. Figure 3(a) gives the cross-sections of the convex slowness surface at different distances from the waveguide axis. From simple geometrical constructions in this figure, it is obvious that only the common guiding velocity profile (with a minimum at the waveguide axis) provides a return of the rays as they move away from the waveguide axis. On the other hand, similar constructions for the cross-sections of the concave slowness surface in figure 3(b) show that the shape of the waveguide ray path (figure 2) can remain basically unchanged only in the case of inversion of the common velocity profile. Thus, the velocity profile required for waveguide mode localization in the case of concave (hyperbolic) anisotropic slowness surfaces evidently appears to be inverse to that needed in the convex slowness case. This simple graphical consideration reveals the basic reason for the uncommon waveguide effect under study. The reason is that the wavevector deflection from the waveguide axis in the concave slowness case produces an inverse deflection of the energy fluxes and respectively of the wave rays from the same axis. At the interface of different media, such a deflection can give rise to the phenomenon of negative refraction, which is the focus of current studies in physics [40–42]. So the reason for the effect under study is, in principle, the same as that for the phenomenon of negative refraction due to anisotropy.

The qualitative analysis of the wave rays presented is valid in general for the concave and convex parts of the slowness surfaces of arbitrary shape. For simple models of

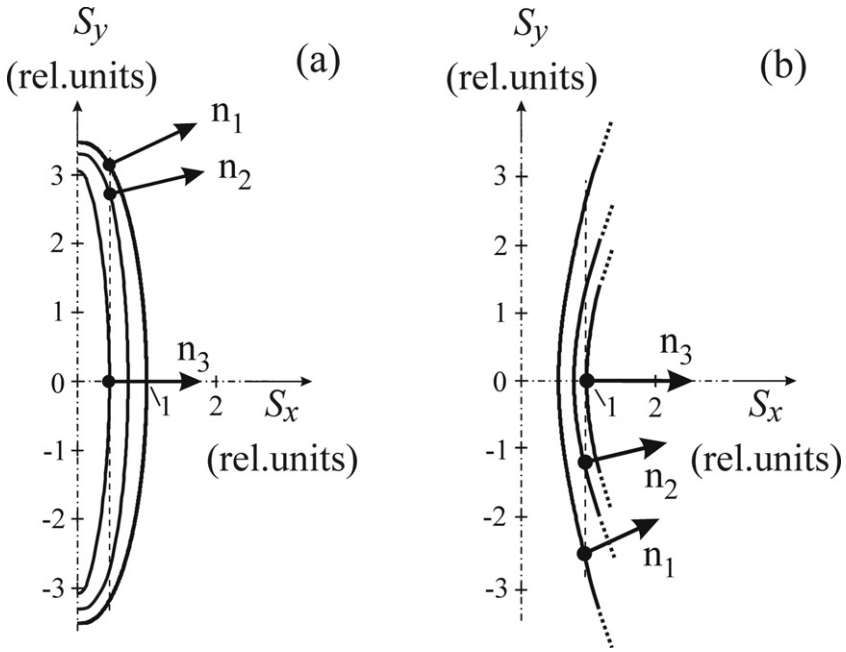

Figure 3. (a) Convex and (b) concave slowness curves (S) at different distances from the waveguide axis. The constructions of rays n_1, n_2, and n_3, corresponding to those in figure 2, are shown.

anisotropy this analysis can be strengthened by developing a quantitative theory, as is done below. To simplify such a theory, the convex and concave parts of the slowness cross-sections are approximated locally using elliptic and hyperbolic curves corresponding to the models considered in the previous section. For both of them, the secular equation following from equation (1) is

$$C_x k_x^2 + C_y k_y^2 = \rho\omega^2, \tag{6}$$

where k_x and k_y are the coordinate projections of the wavevector, $k_x = k\cos\theta_{\rm ph}$, $k_y = k\sin\theta_{\rm ph}$, and $\theta_{\rm ph}$ is the phase velocity angle. In further analysis we adopt the well-known general scheme of ray construction in anisotropic media [43, 44] to our particular problem. The wave ray paths are found using the equation of the tangent to a path

$$\frac{{\rm d}y}{{\rm d}x} = \tan\theta_{\rm gr}, \tag{7}$$

where $\theta_{\rm gr}$ is the ray angle (angle of the group velocity direction), with $\theta_{\rm gr} = \theta_{\rm ph} + \psi$. The angle ψ between the group and the phase velocities is calculated from the angular dependence of the wavenumber $k(\theta_{\rm ph})$ by the well-known formula

$$\tan\psi = -\frac{1}{k}\frac{\partial k}{\partial\theta_{\rm ph}}. \tag{8}$$

Using the expression $k^2 = \rho\omega^2/(C_x\cos^2\theta_{\rm ph} + C_y\sin^2\theta_{\rm ph})$, which follows from equation (6), equation (8) is rewritten as

$$\tan\psi = \frac{(A-1)\tan\theta_{\rm ph}}{1 + A\tan^2\theta_{\rm ph}}. \tag{9}$$

Note that the components of the wavevector are related to $\theta_{\rm ph}$ by the obvious formula

$$\tan\theta_{\rm ph} = k_y/k_x. \tag{10}$$

Now the right hand side of equation (7) can be transformed using equations (9), (10)

$$\tan\theta_{\rm gr} = \tan(\theta_{\rm ph} + \psi) = \frac{\tan\theta_{\rm ph} + \tan\psi}{1 - \tan\theta_{\rm ph}\tan\psi} = A\frac{k_y}{k_x}. \tag{11}$$

Further, eliminating k_y from equation (11) by the use of equation (6) and substituting the relation (2) gives

$$\frac{{\rm d}y}{{\rm d}x} = \sqrt{A\left[\frac{k_0^2}{k_x^2}\left(1 - \gamma_2 y^2\right) - 1\right]}. \tag{12}$$

Finally, the ray paths are found by integrating equation (12)

$$y = \sqrt{\frac{1 - k_x^2/k_0^2}{\gamma_2}}\sin(x/x_0 - C), \tag{13}$$

where $x_0^{-1} = \sqrt{A\gamma_2\frac{k_0^2}{k_x^2}}$, and C is a constant of integration, the value of which defines the position of the ray paths with respect to the coordinate system. Equation (13) is used in calculating the ray path shown in figure 2. In the isotropic limit, this equation coincides with equation (3.9) derived in [8].

The admissible values of the propagation constant k_x involved in equation (13) vary for waveguide modes of different order n. They are denoted further as k_x^n and are found in the ray theory from the condition of transverse resonance

$$4\int_0^{y_0} k_y\,{\rm d}y + 2\Delta\varphi = 2\pi n, \tag{14}$$

where $\Delta\varphi$ is the phase shift at the ray turning point y_0. This shift, as it is known, is equal to $-\pi/2$ [11], and the value of y_0 is found from the condition $k_y(y_0) = 0$, which gives

$$y_0 = \sqrt{\frac{1}{\gamma_2}\left(1 - \frac{(k_x^n)^2}{k_0^2}\right)}. \tag{15}$$

The result of the calculation of k_x^n using equations (14) and (15) is the following

$$k_x^n = \sqrt{k_0^2 - (2n+1)\,{\rm sgn}(A)\sqrt{A\gamma_2 k_0^2}}. \tag{16}$$

As in the isotropic case [45], the ray solution (16) yields the same propagation constants as the exact wave solution (4). Therefore, our previous conclusions, based on elliptic and hyperbolic wave models, about the effect of anisotropy on the guiding velocity profile are also valid for this ray analysis. Thus, the quantitative ray theory, developed in this section, confirms the above prediction of the velocity profile required for waveguide localization in both the cases of convex and concave slowness surfaces. It shows that for the concave surface the profile should be inverse with respect to the common waveguide profile. Note the important difference between waveguide ray paths in media with 'antiguiding' and guiding velocity profiles. In the case of the 'antiguiding' profile, the travel time along the waveguide axis is shorter than for any other ray path, including waveguide ones, and this relation is quite the opposite to that known for the common guiding profile [13].

4. Exact particular solution for guided quasi-shear waves

The analysis presented above is based on a simplified theoretical model of the concave slowness surface. On the other hand, the results of this approximate analysis would be much more convincing if they were supported by an exact calculation. For this reason, an attempt is made here, and in the next section, to find particular exact solutions, with the aim to give a reliable insight into the waveguide mode behavior in the case of a concave slowness surface. In both sections we look for the conditions under which the Gaussian profile is an exact solution for the transverse distribution of the wave field of the guided modes. In this section we consider the problem of waveguide localization for quasi-shear bulk acoustic waves in a graded tetragonal crystal. Let the waves propagate in the vicinity of the crystallographic axis X in such a crystal. For simplicity, a two-dimensional (2D) problem of acoustic beam

propagation in the XY plane is analyzed. The two coupled equations of motion, relevant to the problem, are [24]

$$\rho\ddot{u}_x = c_{11}\frac{\partial^2 u_x}{\partial x^2} + c_{66}\frac{\partial^2 u_x}{\partial y^2} + (c_{12}+c_{66})\frac{\partial^2 u_y}{\partial x\partial y}, \tag{17}$$

$$\rho\ddot{u}_y = c_{66}\frac{\partial^2 u_y}{\partial x^2} + c_{11}\frac{\partial^2 u_y}{\partial y^2} + (c_{12}+c_{66})\frac{\partial^2 u_x}{\partial x\partial y}, \tag{18}$$

where c_{11}, c_{12}, c_{66} are the elastic stiffnesses; u_x, u_y are the displacement vector components; and ρ is the variable mass density defined by equation (2). For cubic crystals, equations (17) and (18) are not changed, only c_{66} is replaced by c_{44}. Note that the stiffness of the crystals is a fourth-rank tensor. This distorts the shape of the acoustic slowness surface and can lead to the appearance of local concavities affecting the waveguide localization.

Searching for the solution to equations (17) and (18) in the form

$$u_y = u_{y0}\exp(-\alpha y^2/2)\exp(\mathrm{i}k_x x - \mathrm{i}\omega t),$$

$$u_x = u_{x0}k_x y\exp(-\alpha y^2/2)\exp(\mathrm{i}k_x x - \mathrm{i}\omega t)$$

results in the following 4 relations, obtained by equating to zero the coefficients of terms with the same power of y,

$$\rho_0\omega^2\gamma_2 = c_{66}\alpha^2, \tag{19}$$

$$\rho_0\omega^2 U = 3c_{66}\alpha U + c_{11}Uk_x^2 + \mathrm{i}(c_{12}+c_{66})\alpha, \tag{20}$$

$$\rho_0\omega^2\gamma_2 = c_{11}\alpha^2 - \mathrm{i}(c_{12}+c_{66})\alpha U k_x^2, \tag{21}$$

$$\rho_0\omega^2 = c_{11}\alpha + c_{66}k_x^2 - \mathrm{i}(c_{12}+c_{66})Uk_x^2, \tag{22}$$

where $U = u_{x0}/u_{y0}$. Equations (19)–(22) are consistent if considered as a system in 4 unknowns instead of the 3 natural ones, such as k_x, α and U. Let us take the coefficient γ_2 as an additional unknown. Then excluding γ_2 from equation (21) by the use of equation (19) reduces the system to 3 equations, the solution to which is

$$k_x^2 = \frac{2k_{0B}^2}{3-A_B}, \tag{23}$$

$$\alpha = k_{0B}^2\frac{1-A_B}{3-A_B}, \tag{24}$$

$$U = \frac{\mathrm{i}}{2}\frac{c_{11}-c_{66}}{c_{12}+c_{66}}(A_B-1), \tag{25}$$

where $k_{0B}^2 = \rho_0\omega^2/c_{66}$, $A_B = c_{11}/c_{66} - (c_{12}+c_{66})^2/[c_{66}(c_{11}-c_{66})]$ is the anisotropy parameter for quasi-shear bulk waves. Similarly to the parameter $A = C_y/C_x$ defined above, A_B has the meaning of the ratio of the effective elastic constants involved in a paraxial wave equation [32] and it determines the shape of the slowness curve near the X axis. For single-component crystals A_B has a wide range of discrete values. On the other hand, for multicomponent crystals there is a possibility to control and to change continuously the value of this parameter, and respectively the slowness surface shape with a smooth transition from local concavity to convexity, by varying the concentration of one of the components. In the isotropic case when $A_B = 1$, the localization of the solution disappears, i.e. $\alpha = 0$, and the obtained solution is transformed into non-localized plane pure shear waves. As follows from equations (23) and (24), the localized solution exists in the range $A_B < 1$, including negative A_B. This range of values admits cases of both convex and concave slowness curves. The curve is convex when $0 \leqslant A_B \leqslant 1$. It becomes locally concave if $A_B < 0$ and it is locally straight at $A_B = 0$. In the last case $k_x(A_B = 0) = k_{0B}\sqrt{2/3} \neq k_{0B}$, i.e. the point corresponding to the propagation constant of quasi-shear waveguide mode does not lie on the flat part of the slowness curve, in contrast to the solution of the simplified wave models, equation (16). For this reason, the singular compression of the waveguide beams found for the elliptical and hyperbolic anisotropy models is eliminated in this exact solution: $\alpha(A_B = 0) = k_{0B}^2/3$, i.e. α is finite at $A_B = 0$. In addition, as is evident from equation (19), the obtained solution describes the waveguide localization in a medium with a common velocity profile, for which $\gamma_2 > 0$ in both the cases of convex and concave slowness. An example of the solution is given in figure 4, where the profiles of local wave velocity v ($v/v_0 = 1/\sqrt{1-\gamma_2 y^2}$) and of waveguide mode field u ($u = u_y$) are shown in an inhomogeneous bulk medium of aluminum-crystal type ($A_B \approx 0.35$). The slowness curve near the waveguide axis is convex in this example. But even when it becomes concave, the velocity profile required for waveguide localization in this solution, according to our analysis, is not changed and it is the same as shown in figure 4. Thus, the above hypothesis about the existence of a localized solution under 'antiguiding' conditions is not confirmed in this particular case.

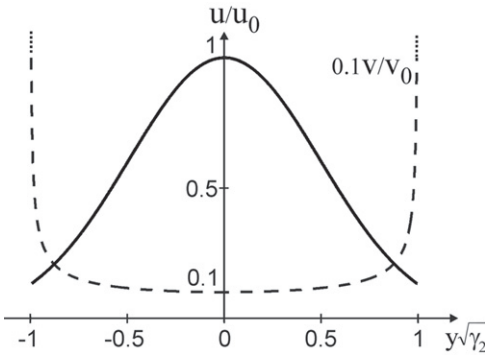

Figure 4. Transverse profiles of local wave velocity v (dashed line) and of wave field $u = u_y$ (full line) for a quasi-shear waveguide mode in an aluminum-type bulk crystal. The curves are normalized by the peak values v_0 and u_0.

5. Exact particular solution for guided flexural waves

In this section we consider localized flexural wave propagation in inhomogeneous thin crystal plates with the aim to find an exact particular analytical solution to this problem. Note that the classical 2D thin plate equation is asymptotically exact as the plate thickness tends to zero. The important point is that this equation is obtained from the 3D equations of elasticity theory by integrating them only over the plate thickness h [46]. Therefore, a gradual variance of the mass density in the lateral direction has no effect on this derivation. Thus,

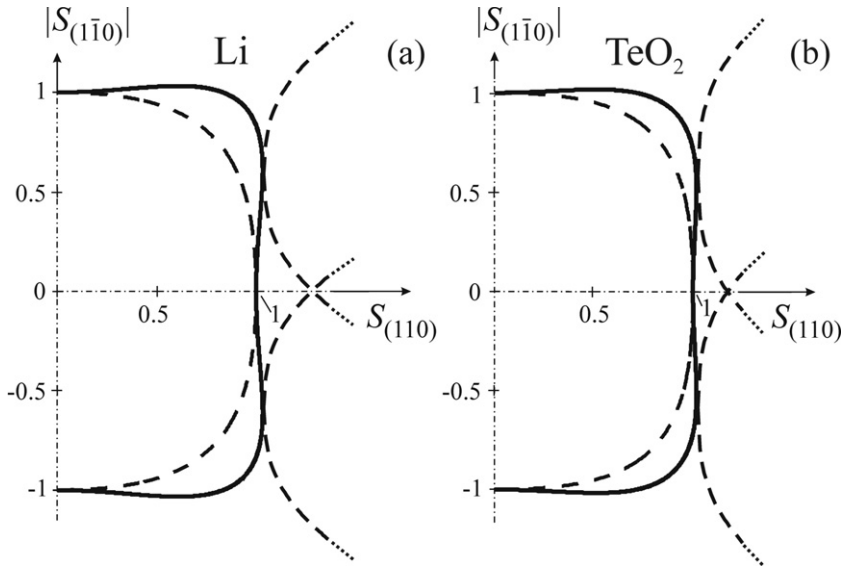

Figure 5. Real and complex branches of the slowness curves (S) for flexural waves in crystal plates of (a) lithium and (b) tellurium dioxide. The real branches are given by full lines and the complex branches by dashed lines.

the equation of thin plates with spatially uniform material parameters is applicable also to the case of thin samples with lateral inhomogeneity in the mass density. For tetragonal crystals of basal-plane cut it reduces to the form [46]

$$\frac{\partial^4 w}{\partial x^4} + A_{\mathrm{F}} \frac{\partial^4 w}{\partial x^2 \partial y^2} + \frac{\partial^4 w}{\partial y^4} + B\rho \ddot{w} = 0, \tag{26}$$

where $A_{\mathrm{F}} = 2(c_{12} + 2c_{66} - c_{13}^2/c_{33})/(c_{11} - c_{13}^2/c_{33})$ is the anisotropy parameter for flexural waves, $B = 12/[h^2(c_{11} - c_{13}^2/c_{33})]$; c_{13}, c_{33} are the elastic stiffnesses, and w is the flexural displacement of the plate. Equation (26) is also valid for cubic crystals if the additional relations are fulfilled: $c_{33} = c_{11}$, $c_{13} = c_{12}$, $c_{66} = c_{44}$. Rotation of the coordinate axes through angle of 45° about the Z axis has no effect on the form of equation (26), changing only the coefficients A_{F} and B. In the rotated coordinates they are

$$A_{\mathrm{F}}(45°) = (3c_{11} - c_{12} - 2c_{66} - 2c_{13}^2/c_{33})/(c_{11} - c_{13}^2/c_{33}),$$

$$B(45°) = 12/[h^2(c_{11} - c_{13}^2/c_{33})].$$

For plane harmonic waves of the form $w \sim \exp(\mathrm{i}k_x x + \mathrm{i}k_y y - \mathrm{i}\omega t)$, equation (26) with constant ρ yields the following secular relation

$$F(k_x, k_y) \equiv k_x^4 + A_{\mathrm{F}} k_x^2 k_y^2 + k_y^4 - \rho\omega^2 B = 0. \tag{27}$$

The transition from the convex to concave slowness surface occurs in the case when all the roots k_y of equation $\partial k_x/\partial k_y = 0$ correspond to the single value of k_x^2. Using an additional formula $\partial k_x/\partial k_y = \partial F/\partial k_y(\partial F/\partial k_x)^{-1}$, one obtains

$$\frac{\partial F}{\partial k_y} = 2k_y(A_{\mathrm{F}} k_x^2 + 2k_y^2) = 0. \tag{28}$$

According to equation (27), the roots k_y of equation (28) correspond to the same value of k_x^2 only in the case when $A_{\mathrm{F}} = 0$, then all these roots are equal to zero. In this case the slowness curve for the flexural waves in the plate plane is convex as a whole but its curvature on the X axis is equal to zero, i.e. the curve is locally straight. The slowness curve becomes concave in the X axis direction if the maxima of the function $k_x(k_y)$ exist at $k_y \neq 0$. This is fulfilled, according to equations (27) and (28), when $A_{\mathrm{F}} < 0$. In the particular case of cubic crystals the inequality $A_{\mathrm{F}} < 0$ gives the two conditions of the slowness concavity derived previously by Every and Maznev [47] for flexural waves propagating in the vicinity of the (100) and (110) directions. Such local concavities are known to exist in the Z-cut crystal plates of cubic lithium and tetragonal tellurium dioxide near the (110) propagation direction [47]. Note that $A_{\mathrm{F}}(45°) < 0$ for both of these crystals: for lithium $A_{\mathrm{F}}(45°) = -2.25$ and for tellurium dioxide $A_{\mathrm{F}}(45°) = -0.27$. The corresponding slowness curves are depicted in figures 5(a) and (b) in rotated coordinates through angle of 45° about the Z axis. In addition to the real branches of the slowness, the complex and imaginary branches are shown. These additional branches are also of interest, since they carry information about the evanescent wave field distribution beyond the turning points of the wave rays. Note that similar concavities in slowness curves, but with strong frequency dependence, are also known for flexural waves in phononic crystal plates [48].

We show now that the waveguide Gaussian beam can be an exact solution to the flexural wave equation in the case of an 'antiguiding' velocity profile. Let the flexural waves propagate in the vicinity of the X axis in the plate and its mass density ρ depend on the lateral coordinate y as

$$\rho(y) = \rho_0(1 - \gamma_4 y^4), \tag{29}$$

where ρ_0 and γ_4 are constant. Note that this profile differs from the one given by equation (2) and used in the previous sections. In the case of a mass load on one side of the plate with

a layer with mass density ρ_l and thickness h_l, $\rho(y)$ is replaced by the sum $\rho + \rho_l h_l/h$ [49]. This means that the transverse velocity profile needed for the waveguide trapping of flexural waves can be realized not only by variations of the crystal mass density but also by variations of the layer thickness, $h_l = h_l(y)$. The last possibility might provide a simpler experimental implementation of a plate with a prescribed profile of the flexural wave velocity. In phononic and photonic crystals, the local wave velocity may be controlled also by a gradual variation of the structural elements [50].

The solution to equation (26) is searched for as $w = w_0 \exp(-\alpha y^2/2) \exp(\mathrm{i}k_x x - \mathrm{i}\omega t)$. This gives the following 3 relations, obtained by equating to zero the coefficients of terms with the same powers of y,

$$k_x^4 + 3\alpha^2 + A_F \alpha k_x^2 - k_{0F}^4 = 0, \tag{30}$$

$$k_x^2 = -6\alpha/A_F, \tag{31}$$

$$\alpha^4 + B\rho_0\omega^2\gamma_4 = 0, \tag{32}$$

where $k_{0F}^4 = B\rho_0\omega^2$. The system of 3 equations (30)–(32) is consistent if it defines 3 unknowns. Let us take k_x, α and γ_4 as these unknowns. It means that a particular mass density profile is considered in this case with value of γ_4 which is not initially fixed, but is determined instead by the other parameters of the problem (including the coefficient A_F). The coefficient γ_4 is involved only in equation (32), which is used to find its value. It is of prime importance for confirmation of the prediction of the present study that the sign of γ_4, as follows from equation (32), happens to be negative. This sign corresponds to a mass density increase and a respective decrease in the velocity when moving from the waveguide axis, i.e. to the velocity profile which is commonly assumed to be 'antiguiding'. Equation (31) shows that the localized solution in search exists only if $A_F < 0$, i.e. in the concave slowness case. Excluding k_x from equation (30) by the use of equation (31), one obtains

$$\alpha^2 = \frac{k_{0F}^4}{3(12/A_F^2 - 1)}. \tag{33}$$

Substitution of equation (33) into equation (31) gives

$$k_x^2 = \frac{k_{0F}^2}{\sqrt{1 - A_F^2/12}}. \tag{34}$$

It follows from equation (33) that: (i) the coefficient α is real if the admissible values of A_F are restricted by the inequality $|A_F| < \sqrt{12}$ and (ii) $\alpha \approx |A_F|(k_{0F}^2/6)$ as A_F tends to zero. Therefore, the absolute beam compression rate, which is proportional to α, decreases in this limiting case. However, the profile of the mass density also changes with decreasing $|A_F|$ so that the density gradient tends to zero. In order to understand better the effect of anisotropy on this solution it is reasonable to consider the relative compression of the waveguide beam along a rescaled lateral coordinate $\tilde{y} = y\sqrt[4]{|\gamma_4|}$. In the rescaled coordinates the mass density profile remains fixed and does not depend on anisotropy, and the lateral dependence of the Gaussian mode field is written as $w \sim \exp(-\tilde{\alpha}\tilde{y}^2/2)$, where $\tilde{\alpha} = \alpha/\sqrt{|\gamma_4|}$ is the relative compression coefficient of the waveguide beam. As follows from equation (32), $\tilde{\alpha} \sim 1/\alpha$, i.e. $\tilde{\alpha} \sim 1/|A_F|$ when $|A_F| \to 0$. Hence, the relative compression of the waveguide beam singularly increases, contrary to the absolute compression that decreases, as the curvature of the slowness concavity tends to zero. Such a conclusion is in full agreement with the results when considering the simplified elliptic and hyperbolic models in sections 2 and 3.

An additional analysis of the waveguide beam angular spectrum could provide a better insight into the effect of anisotropy on the wave field. First note that, according to equation (34), $k_x \to k_{0F}$ as $|A_F| \to 0$, that is, the propagation constant of the waveguide mode approaches the quasi-straight part of the slowness curve in this case. Then the absolute value of the Gaussian beam width, characterized by the factor $\alpha^{-1/2} \sim |A_F|^{-1/2}$, increases, which means that the width of the beam angular spectrum diminishes. On the other hand, the narrower the spectrum is, the less the slowness curve features (for directions far from the waveguide axis) affect the beam parameters. Therefore, the quasi-straight part of the slowness curve plays the dominant role in defining the properties of the solution in the limit $|A_F| \to 0$. This explains the singular increase of the relative compression of the waveguide beam discussed above. Note that although the plane-wave expansion of wave beams is not rigorous in inhomogeneous media, approximately one can apply it here since the medium inhomogeneity (defined by the coefficient γ_4) tends to zero in the limiting case under consideration.

The results of this analysis are confirmed by numerical calculations of local velocity and wave field profiles, shown in figure 6, for crystals of lithium and tellurium dioxide. Note that in this figure, in contrast to figure 4, the velocity v is given by the other formula (here $v/v_0 = 1/\sqrt{1 - \gamma_4 y^4}$). The slowness curvature of tellurium dioxide near the selected waveguide axis is less than that of lithium (see figure 5), which leads, as one can see both from figure 6 and the presented analysis, to the decrease of the transverse width of the waveguide mode corresponding to this crystal. The velocity profiles shown in figures 4 and 6 give an illustrative graphical representation of the difference between the known and new (established by us) guiding conditions.

Thus, the exact analytic solution for flexural waves, obtained in this section, describes the localized waveguide modes in the case of an 'antiguiding' velocity profile in anisotropic graded media with local slowness concavities. In fact, this 'antiguiding' profile becomes guiding, because in the studied case it produces the waveguide effect. For the obtained solution, the relative width of the waveguide beam decreases singularly as the local curvature of the slowness curve tends to zero. These two properties of the exact solution found confirm the predictions of the simplified models elaborated in sections 2 and 3.

6. Comparison of exact solutions

To understand the opposite properties and the predictions of the exact solutions obtained it is reasonable to perform their

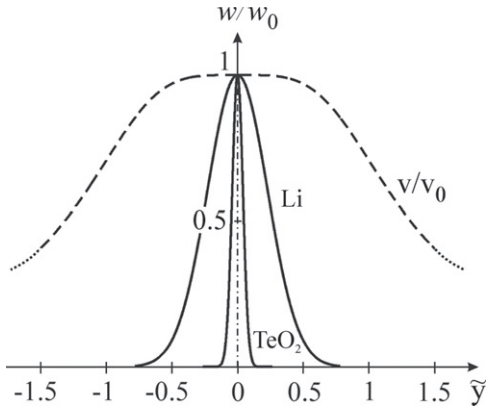

Figure 6. Transverse profiles of local wave velocity v (dashed line) and wave field w (full lines) for flexural waveguide modes in crystal plates of lithium and tellurium dioxide. The dimensionless horizontal coordinate $\tilde{y} = y\sqrt[4]{|\gamma_4|}$ is selected in such a way that the velocity profiles for both crystals in this representation are the same.

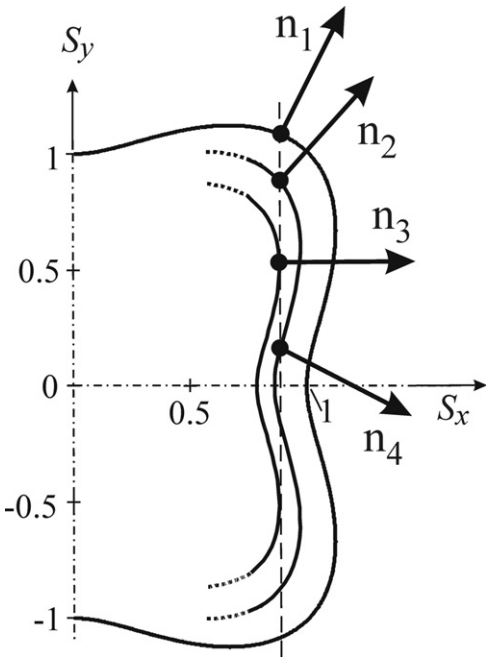

Figure 7. Slowness (S) cross-section evolution for the localized quasi-shear modes at different distances from the waveguide axis. The construction of rays n_1, n_2, and n_3, corresponding to the ray path for guided modes shown in figure 2, is given. The relevance of the n_4 type rays on the concave part of the slowness curve to the waveguide solution found is discussed in the text.

comparative analysis using the slowness surfaces to define the corresponding orientations of the wave rays.

As already noted, the exact solution for localized quasi-shear bulk waves exists in both the cases of convex and concave slowness surfaces. In the case of convexity the common waveguiding velocity profile is required for the existence of this solution, in agreement with the analysis presented in sections 2 and 3. This point is clearly illustrated by the ray constructions in figure 3(a). When the concavity appears, the propagation constant of the quasi-shear waveguide mode k_x does not change its previous position with respect to the value of k_{0B}, which is the propagation constant for wave rays lying on the waveguide axis and traveling along this axis. The recognition of this fact is crucial for understanding the properties of the solution found. Indeed, according to equation (23), k_x is always less than k_{0B}. The same relationship is also valid for the slownesses. As a result, the vertical line corresponding to the slowness of the waveguide modes is shifted leftward with respect to the local concavity of the slowness curve. This is illustrated in figure 7, where the slowness curves are given at different distances from the waveguide axis in a model cubic crystal. The curves are calculated using the secular equation that follows from equations (17) and (18), with stiffness ratios $c_{11}/c_{44} = 0.5$ and $c_{12}/c_{44} = 0.49$, for which the concavity is quite pronounced. Due to the mentioned shift of the slowness, the rays related to the concave part of the slowness surface on the waveguide axis are excluded from the solution, as discussed below. For the common velocity profile, the slowness surface gradually shrinks with increasing distance from the waveguide axis, causing a continuous bending of wave rays from n_1 to n_2, and from n_2 to n_3, demonstrated in figure 7. Beginning from some distance, the dashed vertical line in this figure intersects the concavity, giving rise to rays on the concave part similar to the ray n_4, in addition to rays like n_2 on the convex part. Since it is unlikely that the solution exhibits a jump-like transition from rays of n_2 type to rays of n_4 type, it is reasonable to expect that the found wave solution does not incorporate the rays corresponding to the concave part of the slowness. This explains why the concavity does not change the type of velocity profile for the quasi-shear wave solution, and why it is the same as the well-known guiding profile in the isotropic and convex anisotropic cases.

Nevertheless, this explanation does not mean that the existence of a localized solution is prohibited in the general case for an 'antiguiding' velocity profile. Such an unusual opportunity, as found in section 5, can indeed be real for flexural waves in crystal plates. In this case it is important that, contrary to the localized quasi-shear waves, the propagation constant k_x for the localized flexural waves, according to equation (34), is always more than the propagation constant k_{0F} for wave rays lying on the waveguide axis and traveling along this axis. For this reason, the rays related to the concave part of the slowness curve are now included into the solution. The same situation occurs in the hyperbolic model, for which the required velocity profile is always inverse with respect to the common waveguiding profile.

The discussed solutions also differ essentially from each other in their behavior in the limit when the slowness surface becomes locally flat. For quasi-shear waves, in contrast to the elliptic and hyperbolic models, the waveguide beam compression does not occur in this limit. On the other hand, for flexural waves such compression takes place with respect to the relative beam width. This difference is evidently related to the fact that for flexural waves the slowness curve point corresponding to the waveguide mode appears on the flat part of the curve and for quasi-shear waves this point lies on the convex part. Thus, the apparent contradictions and different properties of the exact particular solutions found for localized

bulk and flexural waves are quite explainable and they are the implications of the variety of the wave phenomena in the studied systems.

In order to understand the cause of disagreement between the exact particular solution of equations (17) and (18) for quasi-shear waves and that of equation (1) for the hyperbolic wave model, it is reasonable to verify whether the first of these two solutions satisfies the condition of the paraxial approximation $|\partial u_i/\partial y| \ll |\partial u_i/\partial x|$, which makes it possible to derive equation (1) from equations (17) and (18) [32]. For the Gaussian profile the mentioned condition reduces to the inequality

$$\alpha y \ll k_x. \tag{35}$$

Although (35) is evidently violated when y becomes large enough, for such well confined wave beams as the Gaussian one it is sufficient to require that this inequality holds at least within the beam boundaries at $y_w = 2/\sqrt{\alpha}$. Substituting y_w and the relations (23), (24) for k_x^2 and α into (35) gives $A_B \gg 1/2$. Such a condition occurs only in the case of a convex slowness surface, but according to the solution (4) it corresponds to the common velocity profile. Therefore, the origin of disagreement between the exact solutions to equations (17), (18) and (1) obviously lies in the failure of the paraxial approximation.

It is worth noting, at the end of this comparison, that while for the elliptic and hyperbolic models the mass density profiles differ only in the sign of the coefficient γ_2, for quasi-shear and flexural waves these profiles are also distinguished from each other by the functional dependencies on y. In addition, the uncommon velocity profile found for flexural waves has no such essential physical restriction on the waveguide area width as does that of the common parabolic profile, as mentioned in section 2.

7. Conclusions

This paper contains prediction of a new, previously unknown physical effect of waveguide localization under conditions which are commonly considered as 'antiguiding'. This unexpected and paradoxical, at first view, effect may occur if the slowness surface of anisotropic wave medium is concave in the direction of wave propagation. Such conditions may be realized for acoustic waves in graded materials, which are attracting a great deal of attention at the present time.

The results obtained can be summarized as follows:

(1) The study of pure shear wave propagation in graded crystals predicts the anisotropy-induced enhancement of the transverse compression of the waveguide modes as the slowness surface curvature decreases in the case of a common guiding velocity profile (where the phase velocity grows with increasing distance from the waveguide axis). This result is absolutely reliable and correct since both the equation of motion and its solution for pure shear waves characterized by the elliptic anisotropy are exact.

(2) The hyperbolic anisotropy model predicts the existence of localized waveguide modes under 'antiguiding' conditions, i.e. when the phase velocity drops rather than grows with increasing distance from the waveguide axis. This model also predicts the strong transverse compression of the waveguide beam as the slowness surface curvature tends to zero.

(3) Both the qualitative and quantitative ray considerations are consistent with the predictions of the elliptic and hyperbolic anisotropy models. The ray formula for the propagation constants of the waveguide modes coincides completely with the corresponding formula of the exact wave solution.

(4) The exact particular solution obtained for localized quasi-shear bulk waves in cubic and tetragonal crystals does not confirm the predictions of the simplified elliptic and hyperbolic anisotropy models, and at first view it contradicts them. However, a more detailed analysis explains this apparent contradiction.

(5) The exact particular solution obtained for flexural waves in thin crystal plates confirms the prediction of the simplified hyperbolic model. It describes the existence of laterally localized waves under 'antiguiding' conditions, that is, when the phase velocity decreases away from the waveguide axis.

Thus, the three diverse approaches to studying the predicted effect, such as using (i) exact general solutions to simplified wave models, (ii) ray analysis, and (iii) exact particular solutions to the more complicated wave models, make the prediction clear, convincing and reliable. It is worth noting that the exact solution found for flexural waves is substantially different, with respect to the existence conditions, from all others yet reported and it cannot be deduced from the previously known results. Therefore, the predicted waves can be classified as a new type of waveguide mode in graded anisotropic media with an 'antiguiding' velocity profile. The present study does not completely deny the previous general notion about waveguide localization conditions in inhomogeneous media, but it shows its limited applicability in media with special anisotropic properties. Although the above consideration concerns acoustic waves, one can expect the occurrence of the predicted effect for waves of different natures including, in particular, plasma, spin and optical waves, under conditions such that the medium anisotropy produces slowness surface concavities. The results obtained could also offer a new point of view in the development of the theory of streamer breakdown caused by phonon streams in crystals [51]. Further generalizations of the obtained results may be related to the study of similar effects in self-focusing wave beams in nonlinear media.

Acknowledgment

This work was supported in part by the Russian Foundation for Basic Research (project No. 07-02-01201).

References

[1] Birman V and Byrd L W 2007 *Appl. Mech. Rev.* **60** 195–216
[2] Brekhovskikh L M 1960 *Waves in Layered Media* (New York: Academic)
[3] Ewing W M, Jardetzky W S and Press F 1957 *Elastic Waves in Layered Media* (New York: McGraw-Hill)
[4] Babich V M and Buldyrev V S 2008 *Asymptotic Methods in Short-Wavelength Diffraction Theory* (Oxford: Alpha Science International)
[5] Chew W C 1990 *Waves and Fields in Inhomogeneous Media* (New York: Van Nostrand-Reinhold)
[6] Eckart C 1960 *Hydrodynamics of Oceans and Atmospheres* (Oxford: Pergamon)
[7] Haus H A 1984 *Waves and Fields in Optoelectronics* (Englewood Cliffs, NJ: Prentice-Hall)
[8] Adams M J 1981 *An Introduction to Optical Waveguides* (New York: Wiley)
[9] Cerveny V 2001 *Seismic Ray Theory* (Cambridge: Cambridge University Press)
[10] Slawinski M A 2003 *Seismic Waves and Rays in Elastic Media* (Amsterdam: Pergamon)
[11] Kravtsov Y A and Orlov Y I 1990 *Geometrical Optics of Inhomogeneous Media* (Berlin: Springer)
[12] Biryukov S V, Gulyaev Yu V, Krylov V V and Plessky V P 1995 *Surface Acoustic Waves in Inhomogeneous Media* (Berlin: Springer)
[13] Brekhovskikh L M and Lysanov Yu P 2003 *Fundamentals of Ocean Acoustics* (New York: Springer)
[14] Yariv A 1971 *Introduction to Optical Electronics* (New York: Holt, Rinehart and Winston)
[15] Kal S 2006 *Basic Electronics: Devices, Circuits and IT Fundamentals* (New Delhi: Prentice-Hall) p 473
[16] Neumann E-G 1987 *J. Opt. Soc. Am.* A **4** 1021–9
[17] Madelung O 1978 *Introduction to Solid-State Theory* (Berlin: Springer)
[18] Kosevich A M 2005 *The Crystal Lattice: Phonons, Solitons, Dislocations, Superlattices* (Weinheim: Wiley-VCH)
[19] Yariv A and Yeh P 1984 *Optical Waves in Crystals* (New York: Wiley)
[20] Felsen L B and Marcuvitz N 1994 *Radiation and Scattering of Waves* (New York: Wiley)
[21] Ginzburg V L 1970 *The Propagation of Electromagnetic Waves in Plasmas* (Oxford: Pergamon)
[22] Vashkovskii A V and Lokk E H 2006 *Usp. Fiz. Nauk* **176** 403–14
Vashkovskii A V and Lokk E H 2006 *Phys. Usp.* **49** 389–99 (Engl. Transl.)
[23] Mizuguchi J, Tanaka Y, Tamura S and Notomi M 2003 *Phys. Rev.* B **67** 075109
[24] Musgrave M J P 1970 *Crystal Acoustics* (San Francisco: Holden-Day Inc.)
[25] Zinin P, Lefeuvre O, Briggs G A D, Zeller B D, Cawley P, Kinloch A J and Thompson G E 1997 *J. Appl. Phys.* **82** 1031–5
[26] Mozhaev V G and Weihnacht M 1998 *J. Korean Phys. Soc.* **32** s747–9
[27] Mozhaev V G and Zyryanova A V 2008 *Phys. Wave Phenom.* **16** 300–4
[28] Mozhaev V G and Zyryanova A V 2009 *Tech. Phys. Lett.* **35** 456–8
[29] Adachi S (ed) 1993 *Properties of Aluminium Gallium Arsenide* (Stevenage: IEE) p 5 and 18
[30] Shearer P M and Chapman C H 1989 *Geophys. J.* **96** 51–64
[31] Ghatak A K and Thyagarajan K 1989 *Optical Electronics* (Cambridge: Cambridge University Press) p 336
[32] Kozlov A V and Mozhaev V G 2006 *Proc. 20th European Frequency and Time Forum (Braunschweig)* pp 33–40
[33] Lanceleur P, de Belleval J F and Mercier N 1998 *Acustica* **84** 1047–54
[34] Laude V, Wilm M and Ballandras S 2003 *J. Appl. Phys.* **93** 10084–8
[35] Laude V, Masson M, Ballandras S and Solal M 2004 *J. Appl. Phys.* **96** 6895–902
[36] Declercq N F, Degrieck J and Leroy O 2005 *Acta Acust. United Acust.* **91** 840–5
[37] Declercq N F, Polikarpova N V, Voloshinov V B, Leroy O and Degrieck J 2006 *Ultrasonics* **44** e833–7
[38] Rogister Y and Slawinski M A 2005 *Geophysics* **70** D37–41
[39] Shearer P M and Chapman C H 1988 *Geophys. J.* **94** 575–80
[40] Felsen L B 1964 *IEEE Trans.* **AP-12** 624–35
[41] Imamura K and Tamura S 2004 *Phys. Rev.* B **70** 174308
[42] Kozlov A V and Mozhaev V G 2008 *Phys. Lett.* A **372** 4718–21
[43] Mullaly R F 1962 *Aust. J. Phys.* **15** 96–105
[44] Jenkins Ch, Bingham R, Moore K and Love G D 2007 *J. Opt. Soc. Am.* A **24** 2089–96
[45] Ankiewicz A 1978 *Opt. Acta* **25** 361–73
[46] Lekhnitskii S G 1987 *Anisotropic Plates* (New York: Gordon and Breach)
[47] Every A G and Maznev A A 1995 *Acta Acust.* **3** 387–91
[48] Wen J, Yu D, Wang G and Wen X 2008 *J. Phys. D: Appl. Phys.* **41** 135505
[49] Kopmaz O and Telli S 2002 *J. Sound Vib.* **251** 39–57
[50] Lin S-C S, Huang T J, Sun J-H and Wu T-T 2009 *Phys. Rev.* B **79** 094302
[51] Chernozatonskii L A 1983 *JETP Lett.* **38** 265–8